J Biomol NMR (2009) 45:301–310
DOI 10.1007/s10858-009-9373-4

ARTICLE

An intraresidual i(HCA)CO(CA)NH experiment for the assignment of main-chain resonances in ^{15}N, ^{13}C labeled proteins

Sampo Mäntylahti · Helena Tossavainen · Maarit Hellman · Perttu Permi

Received: 1 July 2009 / Accepted: 5 August 2009 / Published online: 19 September 2009

Abstract An improved pulse sequence, intraresidual i(HCA)CO(CA)NH, is described for establishing solely $^{13}C'(i)$, $^{15}N(i)$, $^{1}H^{N}(i)$ connectivities in uniformly $^{15}N/^{13}C$-labeled proteins. In comparison to the "out-and-back" style intra-HN(CA)CO experiment, the new pulse sequence offers at least two-fold higher experimental resolution in the $^{13}C'$ dimension and on average 1.6 times higher sensitivity especially for residues in α-helices. Performance of the new experiment was tested on a small globular protein ubiquitin and an intrinsically unfolded 110-residue cancer/testis antigen CT16/PAGE5. Use of intraresidual i(HCA)CO(CA)NH experiment in combination with the established HNCO experiment was crucial for the assignment of highly disordered CT16.

Keywords Assignment · CT16 · HN(CA)CO · (HCA)CO(CA)NH · Proteins · Ubiquitin

Introduction

Assignment of protein main-chain resonances is a critical step in structural and functional studies of proteins by solution state NMR spectroscopy. Hence, considerable effort has been invested in developing and improving both resolution and sensitivity of the employed experiments for the main-chain assignment (For review see e.g. Sattler et al. 1999; Permi and Annila 2004). Although main-chain assignment of ^{15}N, ^{13}C labeled proteins less than ca. 20 kDa can routinely be obtained using a conventional set of triple resonance experiments e.g. HNCA, HN(CO)CA, HNCACB, CBCA(CO)NH, it has been recently shown that intraresidual experiments, exhibiting solely *intraresidual* cross peaks per $^{1}H^{N}/^{15}N$ pair (Brutscher 2002; Nietlispach et al. 2002; Permi 2002), can efficiently be utilized for assignment of both small ^{15}N, ^{13}C labeled and larger ^{15}N, ^{13}C, ^{2}H enriched globular proteins as well as intrinsically unfolded proteins (Nietlispach et al. 2002; Bersch et al. 2003; Alho et al. 2007). Moreover, a set of unidirectional triple resonance experiments e.g. iHNCA/HN(CO)CA, iHN(CA)CB/CBCA(CO)NH, intra-HCCNH/HC(CO)NH (Jiang et al. 2005) are ideal for projection reconstruction applications (Jiang et al. 2005), extensive spectral compression approach (Lescop et al. 2007) or hyper-dimensional spectroscopy with targeted acquisition and automated assignment (Jaravine et al. 2008). All these approaches greatly benefit from minimal cross peak overlap in the spectra, facilitating peak picking especially on sparsely sampled data (Jaravine et al. 2008). Although not very broadly utilized, the chemical shift of $^{13}C'$ spin provides invaluable support for the sequential assignment, resolving ambiguities arising from $^{13}C\alpha/^{13}C\beta$ shift degeneracy (Clubb et al. 1992; Grzesiek and Bax 1992). This is of key importance especially in the case of intrinsically unfolded proteins as $^{13}C'$ chemical shift is less dependent on residue type, rendering chemical shift dispersion in $^{13}C'$ region far more superior to $^{13}C^{\alpha/\beta}$ dimension in unfolded proteins (Yao et al. 1997; Dyson and Wright 2001). Therefore, additional sequential connectivities can be established through $^{13}C'$ chemical shifts using HN(CA)CO/HNCO experiment pair. The former experiment establishes connectivity from amide proton to both *intraresidual* and *sequential* carbonyl carbon, which may transmute the assignment unambiguous

Electronic supplementary material The online version of this article (doi:10.1007/s10858-009-9373-4) contains supplementary material, which is available to authorized users.

S. Mäntylahti · H. Tossavainen · M. Hellman · P. Permi (✉)
Program in Structural Biology and Biophysics,
Institute of Biotechnology/NMR Laboratory, University of Helsinki, P.O. Box 65, 00014 Helsinki, Finland
e-mail: Perttu.Permi@helsinki.fi

especially in unfolded systems. Recently, Nietlispach developed an intra-HN(CA)CO-TROSY experiment (Nietlispach 2004), which create solely intraresidual connectivities in a manner conceptually similar to the intraresidual HNCA experiment. The sensitivity of the experiment is, however, very susceptible to transverse relaxation of $^{13}C^{\alpha}$ spin as $^{1}H^{N}(i)$–$^{13}C'(i)$ connectivities are established through the unidirectional coherence transfer utilizing the multiple-quantum (MQ) coherence between two adjacent $^{13}C^{\alpha}$ spins, which is known to relax notoriously fast even on small proteins (Nietlispach 2004). Consequently, use of intra-HN(CA)CO greatly benefits from highly deuterated $^{13}C^{\alpha}$ sites together with the TROSY implementation (Nietlispach 2004).

In this work, we describe a modified intraresidual pulse scheme that is more suitable for $^{15}N/^{13}C$ labeled proteins than a non-TROSY analog of intra-HN(CA)CO employing a constant-time MQ implementation (Nietlispach 2004). The experiment presented in this work provides at least two-fold enhancement in experimental resolution along $^{13}C'$ dimension, more uniform coherence transfer, and increased sensitivity for small- to medium-sized proteins. We also show that the editing of intraresidual cross peaks can be obtained with high selectivity resulting in a spectrum with purely intraresidual correlations.

Theory

Description of the pulse sequence

The proposed intraresidual i(HCA)CO(CA)NH experiment for establishing correlations between $^{13}C'_i$ and $^{15}N_i/^{1}H_i^{N}$ spins is shown in Fig. 1a, whereas the inset displays a schematic presentation of magnetization transfer during the experiment. The i(HCA)CO(CA)NH scheme is mostly similar to the (HCA)CO(CA)NH experiment, originally introduced by Löhr and Rüterjans (1995) and Bazzo and coworkers (1996), and improved more recently by Tessari et al. (1997) and Folmer and Otting (2000). It also utilizes non-linearity of the N(i)–Cα(i)–C$'$(i)–N($i+1$) spin system to obtain intraresidual filtering (Permi 2002; Jiang et al. 2005).

The flow of initial $^{1}H^{\alpha}$ steady state magnetization during the i(HCA)CO(CA)NH experiment (Fig. 1) can be described in the following way

$$^{1}H^{\alpha} \xrightarrow{^{1}J_{HC}} {}^{13}C^{\alpha}$$
$$\xrightarrow{^{1}J_{C\alpha N},\,^{2}J_{C\alpha N},\,^{1}J_{C\alpha C'}} {}^{13}C'(2T_A - t_1;\,^{1}J_{C'N};\,^{1}J_{C\alpha N};\,^{2}J_{C\alpha N})$$
$$\xrightarrow{^{1}J_{C\alpha N},\,^{2}J_{C\alpha N},\,^{1}J_{C\alpha C'}} {}^{15}N(2T_N - t_2;\,^{1}J_{C\alpha N};\,^{2}J_{C\alpha N}) \xrightarrow{^{1}J_{NH}} {}^{1}H^{N}(t_3)$$

Active couplings, which are employed for the magnetization transfer are indicated above the arrows and in parentheses during the constant time acquisition periods, t_i ($i = 1$–3) refer to the acquisition time for the corresponding spin.

The experiment starts with the INEPT transfer from $^{1}H^{\alpha}(i)$ to $^{13}C^{\alpha}(i)$. At the time point a (see Fig. 1a, b), the density operator is given by

$$\sigma(a) = H_z^{\alpha}(i)C_x^{\alpha}(i).$$

During the ensuing delay T_C and 90°($^{13}C'$) pulse, the magnetization is transferred to directly bound $^{13}C'(i)$ spin while antiphase coherence with respect to $^{1}H^{\alpha}(i)$ spin is refocused. Hence, the density operator at time point b is

$$\sigma(b) = C_x^{\alpha}(i)C_y'(i)\sin(\pi J_{C\alpha C'}(T_C)).$$

Chemical shift of $^{13}C'(i)$ spin is labeled during the constant time period $2T_A$, which is matched to $(2J_{C'N})^{-1}$ $\sim$33 ms in order to create antiphase coherence with respect to the ^{15}N spin of residue $i+1$. Therefore, the density operator describing the spin system at time point c is

$$\sigma(c) = C_x^{\alpha}(i)C_x'(i)N_z(i+1)\cos(\omega_{C'}t_1)\sin(\pi J_{C\alpha C'}(T_C)) \times \sin(2\pi J_{C'N}(T_A)).$$

After labeling the $^{13}C'(i)$ chemical shift, the magnetization will be converted back to $^{13}C^{\alpha}(i)$ single quantum (SQ) antiphase coherence by the 90°($^{13}C'$) pulse (time point c). The coupling between $^{13}C^{\alpha}(i)$ and $^{13}C'(i)$ spins will be refocused during the latter delay T_C yielding density operator at time point d

$$\sigma(d) = C_y^{\alpha}(i)N_z(i+1)\cos(\omega_{C'}t_1)\sin^2(\pi J_{C\alpha C'}(T_C)) \times \sin(2\pi J_{C'N}(T_A)).$$

The homonuclear one-bond coupling between $^{13}C\alpha$ and $^{13}C\beta$ spins remains active between time points a and d resulting in an additional modulation by $\cos(2\pi^{1}J_{C\alpha C\beta}(T_A + T_C + T_{CC}))$, $2(T_A + T_C + T_{CC})$ $\sim$57 ms. The selection of solely *intraresidual* pathway is accomplished by enabling $^{1}J_{C\alpha N}$ and $^{2}J_{C\alpha N}$ coupling modulation throughout the $2(T_A + T_C)$ period and by choosing the sin $(2\pi^{1}J_{C\alpha N}(T_A + T_C)) \times \sin(2\pi^{2}J_{C\alpha N}(T_A + T_C))$ modulated signal via appropriate phase setting. Hence, density operators describing the desired *intraresidual* and undesired *sequential* coherence transfer routes, selected with the 90°($^{13}C^{\alpha}$) pulse at time point e, are

$$\sigma(e) = \{N_z(i)C_z^{\alpha}(i)\Gamma_i(2(T_C + T_A)) + C_z^{\alpha}(i)N_z(i+1)\Gamma_s(2(T_C + T_A))\} \times \cos(\omega_{C'}t_1)\sin(2\pi J_{C'N}T_A)\sin^2(\pi J_{C\alpha C'}T_C) \times \cos(2\pi J_{C\alpha C\beta}(T_A + T_C + T_{CC})),$$

in which $\Gamma_i(a)$ and $\Gamma_i(b)$ are transfer functions leading to intraresidual and sequential correlations, respectively:

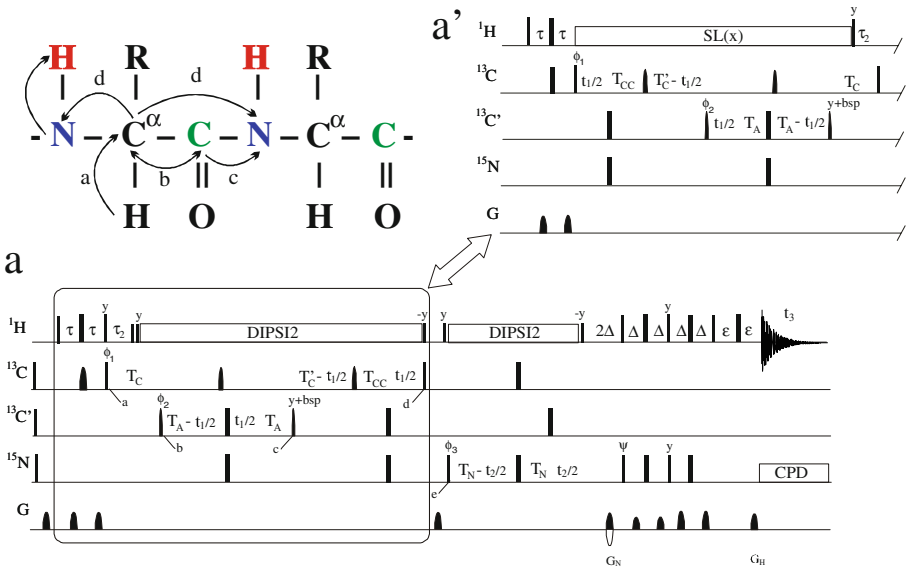

Fig. 1 **a** Intraresidual i(HCA)CO(CA)NH experiment and **a′** spin-lock version of the i(HCA)CO(CA)NH for the assignment of $^{1}H^{N}$, ^{15}N and $^{13}C'$ resonances in $^{15}N/^{13}C$ labeled proteins. The *inset* shows a schematic presentation of magnetization transfer pathway during the intraresidual i(HCA)CO(CA)NH experiment. *One-letter* codes above the *arrows* indicate time points in the pulse sequence. *Narrow* and *wide bars* correspond to 90° and 180° flip angles, respectively, applied with phase *x* unless otherwise indicated. The ^{1}H, ^{15}N, and $^{13}C'$ carrier positions are 4.7 (water), 118 (center of ^{15}N spectral region), and 175 ppm (center of $^{13}C'$ spectral region). The ^{13}C carrier is set initially to the middle of $^{13}C\alpha$ region (57 ppm), shifted to 175 ppm just after the first 90° ^{13}C pulse (time point *a*), and shifted back to 175 ppm after time point *c*. All rectangular 90° pulses for $^{13}C\alpha$ (57 ppm) and 180° pulses for $^{13}C'$ (175 ppm) were applied with durations of 54 μs (90°) and 48.7 μs (180°) at 600 MHz, respectively in order to provide null mutual excitation (Kay et al. 1990). The first 180° pulse for ^{13}C is an adiabatic, band-selective $^{13}C\alpha$ inversion pulse with a sech/tanh profile and duration of 1 ms (Silver et al. 1984; Bendall 1995). Two selective 90° pulses for $^{13}C'$ have the shape of center lobe of a sinc function and duration of 89.2 μs. Phase modulated 180° pulses, applied off-resonance for $^{13}C\alpha$ have the shape of one-lobe the sinc profile and duration of 80.8 μs. The DIPSI-2 sequence (Shaka et al. 1988) with a strength of 4.8 kHz is employed to decouple ^{1}H spins during $2(T_C + T_A + T_{CC}) - \tau_2$ and $2(T_N - \Delta)$ periods. The adiabatic WURST field (Kupće and Wagner 1995) was used to decouple ^{15}N during acquisition. Delay durations: $\tau = 1/(4J_{HC})$ ~1.7 ms; $\tau_2 = 2.4$ or 4.4 ms; $\Delta = 1/(4J_{NH})$ ~2.7 ms; ε = duration of G_H + field recovery ~0.4 ms; $T_C = 1/(2J_{C\alpha C'})$ ~9.5 ms; $T_A = 1/(4J_{C'N})$ ~16.6 ms; $T'_C = T_C + T_{CC}$; $T_{CC} = 1/(J_{C\alpha C\beta}) - 1/(4J_{C'N}) - 1/(2J_{C\alpha C'})$ ~0 − 2.5 ms; $t_{1,max} < T'_C$. Frequency discrimination in $^{13}C'$ dimension is obtained using the States-TPPI protocol (Marion et al. 1989) applied to ϕ_2, whereas quadrature detection in ^{15}N dimension is obtained using the sensitivity-enhanced gradient selection (Kay et al. 1992). The echo and antiecho signals in ^{15}N dimension are collected separately by inverting the sign of the G_N gradient pulse together with the inversion of ψ, respectively. Phase cycling: $\phi_1 = y, -y$; $\phi_2 = 2(x), 2(-x)$, $\phi_3 = x$; $\psi = x$; rec. $= x, 2(-x), x$. Because a selective 180° pulse for $^{13}C\alpha$ in the middle of delay $2T_A$ induces a Bloch–Siegert shift to $^{13}C'$ magnetization, a careful adjustment of phase (bsp) of the last $^{13}C'$ 90°(phase *y*) pulse is necessary. Gradient strengths and durations: $G_N = 13$ k G/cm (2 ms), $G_H = 13$ k G/cm (0.2 ms). The pulse sequence code and parameter file for Varian Inova system are available in supplementary material

$$\Gamma_i(2(T_A + T_C)) = \sin(2\pi^1 J_{C\alpha N}(T_C + T_A)) \times \sin(2\pi^2 J_{C\alpha N}(T_C + T_A));$$

$$\Gamma_s(2(T_A + T_C)) = \cos(2\pi^1 J_{C\alpha N}(T_C + T_A)) \times \cos(2\pi^2 J_{C\alpha N}(T_C + T_A)).$$

The first term leads to the intraresidual cross peak and the latter term on the right hand side corresponds to magnetization leading to the undesired sequential correlations. Because in i(HCA)CO(CA)NH scheme the chemical shift of intraresidual carbonyl carbon is of interest, we use a somewhat different implementation of the intraresidual filtering proposed by Zhou and coworkers (2005). The chemical shift of the $^{13}C'$ spin is labeled during the t_1 evolution period, which is implemented into the constant time delay $2T_A$ (~33 ms). However, owing to a nested t_1 incrementation within the intraresidue filter, the refocusing of $^{13}C\alpha$ chemical shift and one- and two-bond J_{NC} coupling evolution during t_1, constrains the $t_{1,max}$ to $2(T_C + T_{CC})$ ~18–24 ms. The coherence transfer efficiency for intraresidual (sequential) correlations is maximized (minimized) by setting $2(T_C + T_A)$ ~50–52 ms (Permi 2002). Therefore, modulation of $^{1}J_{C\alpha N}$ and $^{2}J_{C\alpha N}$ is taking place during $2(T_C + T_A)$, and $^{1}J_{C\alpha C\beta}$ modulation is effective for $2(T_C + T_A + T_{CC})$. This also enables setting of $2T_A$ to the optimal value of ~33 ms (= $1/2J_{C'N}$). Although the suppression of the sequential pathway is not perfect, it can be diminished at least by a factor of 10–20 (Permi 2002; Jiang et al. 2005) by a judicious choice of the $2(T_C + T_A)$ delay. In case of our test protein, ubiquitin, containing all the secondary structure elements and providing with very high signal-to-noise ratio, no sequential peaks were observed, and hence we can safely

neglect the term leading to a sequential correlation from this point onward.

Figure 1a′ depicts the so-called spin-locked MQ version of the i(HCA)CO(CA)NH experiment. Albeit not experimentally tested here, the MQ coherence created between ^{1}Hα and ^{13}Cα spins quenches their mutual dipolar interaction (Griffey and Redfield 1987), potentially leading to further sensitivity enhancement for non-glycine residues owing to extended transverse relaxation times with respect to the ^{13}Cα SQ coherence (Tessari et al. 1997; Folmer and Otting 2000).

Onward from the point *e*, the i(HCA)CO(CA)NH pulse sequence is identical to the sensitivity enhanced HNCA experiment. Thus, magnetization is transferred to the ^{15}N(i) spin and the one-bond ^{13}C$^{\alpha}$(i)–^{15}N(i) coupling is refocused simultaneously with ^{15}N chemical shift labeling during the ensuing $2T_{\mathrm{N}}$ delay. Standard gradient enhanced coherence order selective coherence transfer is employed for the $^{15}\mathrm{N} \rightarrow {}^{1}\mathrm{H}^{\mathrm{N}}$ transfer. Therefore, after the Fourier transform, a three-dimensional spectrum is obtained showing cross peaks at $\omega_{\mathrm{C}'}(i)$, $\omega_{\mathrm{N}}(i)$, $\omega_{\mathrm{HN}}(i)$ i.e. explicitly intraresidual $^{1}\mathrm{H}^{\mathrm{N}}-^{15}\mathrm{N}-^{13}\mathrm{C}'$ correlations are observed per amino acid residue.

Results and discussion

It is interesting to compare attainable sensitivities of the non-TROSY implementation of the intra-HN(CA)CO and the proposed i(HCA)CO(CA)NH experiment. Theoretical coherence transfer efficiencies for i(HCA)CO(CA)NH and intra-HN(CA)CO schemes are

$$
\begin{aligned}
I_{i(\mathrm{HCA})\mathrm{CO}(\mathrm{CA})\mathrm{NH}} \approx\ & \sin(2\pi^{1}J_{\mathrm{C}\alpha\mathrm{N}}(T_{\mathrm{C}}+T_{\mathrm{A}})) \\
& \times \sin(2\pi^{2}(2\pi^{2}J_{\mathrm{C}\alpha\mathrm{N}}(T_{\mathrm{C}}+T_{\mathrm{A}}))\sin^{2}(2\pi J_{\mathrm{C}\alpha\mathrm{C}'}T_{\mathrm{C}}) \\
& \times \sin(2\pi^{1}J_{\mathrm{C}'\mathrm{N}}T_{\mathrm{A}})\cos(2\pi^{1}J_{\mathrm{C}\alpha\mathrm{C}\beta}(T_{\mathrm{C}}+T_{\mathrm{A}}+T_{\mathrm{CC}})) \\
& \times \sin(2\pi^{1}J_{\mathrm{C}\alpha\mathrm{N}}T_{\mathrm{N}})\cos(2\pi^{2}J_{\mathrm{C}\alpha\mathrm{N}}T_{\mathrm{N}}) \\
& \times \exp(-2(T_{\mathrm{C}}+T_{\mathrm{A}}+T_{\mathrm{CC}})/T_{2,\mathrm{C}\alpha}) \\
& \times \exp(-(2T_{\mathrm{A}})/T_{2,\mathrm{C}'})\exp(-(2T_{\mathrm{A}})/T_{2,\mathrm{N}})
\end{aligned}
$$

and

$$
\begin{aligned}
I_{\mathrm{intra}-\mathrm{HN}(\mathrm{CA})\mathrm{CO}} \approx\ & \sin^{2}(4\pi^{1}J_{\mathrm{NC}\alpha}T_{\mathrm{NC}a})\sin^{2}(4\pi^{2}J_{\mathrm{NC}\alpha}T_{\mathrm{NC}a}) \\
& \times \sin^{2}(2\pi J_{\mathrm{C}\alpha\mathrm{C}}T_{\mathrm{C}})\cos(2\pi J_{\mathrm{C}\alpha\mathrm{C}\beta}(T_{\mathrm{C}}+T_{\mathrm{CC}})) \\
& \times \exp(-2(T_{\mathrm{C}}+T_{\mathrm{CC}})/T_{2,\mathrm{MQ},\mathrm{C}\alpha})\exp(-(4T_{\mathrm{NC}a})/T_{2,\mathrm{N}}) \\
& \times \exp(-(2T_{\mathrm{CC}})/T_{2,\mathrm{C}'}),
\end{aligned}
$$

respectively. The coherence transfer efficiency, neglecting relaxation, for residues in α-helical (β-strand) conformation in i(HCA)CO(CA)NH and intra-HN(CA)CO experiments are ∼0.54 (0.58) and 0.75 (0.91), respectively. Therefore, any theoretical or experimental improvement in sensitivity with respect to the intra-HN(CA)CO must stem from the diminished relaxation of magnetization during the course of i(HCA)CO(CA)NH. Indeed, the overall duration of the proposed i(HCA)CO(CA)NH scheme is ∼50 ms shorter than the intra-HN(CA)CO. Although i(HCA)CO(CA)NH includes a coherence transfer step during which the ^{13}Cα spin is susceptible to transverse relaxation for a period extending up to 57 ms, the ^{13}Cα–^{13}Cα MQ coherence created in the intra-HN(CA)CO scheme is relaxing extremely fast in non-deuterated samples during the constant-time period of $2T_{\mathrm{C}}$ (∼28 ms) (Nietlispach 2004).

Figure 2 shows calculated coherence transfer efficiencies for globular small and medium sized proteins, having rotational correlation times of 5 and 8 ns. For instance, considering a small globular protein with transverse relaxation times for ^{15}N, ^{13}C$^{\alpha}$ and ^{13}C′ spins of 100, 40, 100 ms at 600 MHz, respectively, the transfer efficiencies for residues in α-helical (β-strand) conformation are 29% (8%) higher in i(HCA)CO(CA)NH with respect to the intra-HN(CA)CO experiment. In the above calculations, the relaxation rate of ^{13}C$^{\alpha}$–^{13}C$^{\alpha}$ multiple-quantum coherence is assumed to be twice the relaxation rate of ^{13}C$^{\alpha}$ single-quantum coherence i.e. $R_2\left[{}^{13}\mathrm{C}_x^{\alpha}(i) - {}^{13}\mathrm{C}_x^{\alpha}(i-1)\right] = R_2\left[{}^{13}\mathrm{C}_x^{\alpha}(i)\right] + R_2\left[{}^{13}\mathrm{C}_x^{\alpha}(i-1)\right] \approx 2 \times R_2\left[{}^{13}\mathrm{C}_x^{\alpha}(i)\right]$. For simplicity, the cross-correlation effect between two ^{13}C$^{\alpha}$–^{1}H$^{\alpha}$ dipole–dipole relaxation mechanisms in adjacent residues has been neglected. Hence, in case of smaller proteins where (per)deuteration is not a prerequisite, the proposed i(HCA)CO(CA)NH experiment provides superior sensitivity with respect to the out-and-back style intra-HN(CA)CO scheme especially for residues in α-helical conformation for which the intraresidual coherence transfer is inherently less efficient.

The calculations also indicate that coherence transfer efficiency is more uniform in the case of the i(HCA)CO(CA)NH experiment i.e. similar transfer efficiencies are obtained irrespective of polypeptide conformation. In the case of unfolded polypeptide chain e.g. natively disordered protein with R_2 values for ^{15}N as low as 3–5 s^{-1}, the transfer efficiencies for i(HCA)CO(CA)NH and intra-HN(CA)CO are ∼0.24 and 0.29, respectively, assuming ^{1}J and ^{2}J couplings between Cα and N to be 10.6 and 7.5 Hz (Delaglio et al. 1991). Although the absolute transfer efficiency in the case of unfolded polypeptide with extremely long relaxation times is higher for the intra-HN(CA)CO, the transfer efficiency for the emerging or transient α-helical conformation is almost equal between i(HCA)CO(CA)NH and intra-HN(CA)CO. These regions, having tendency for nascent secondary structure, exhibit shorter transfer relaxation times reminiscent of those observed for globular proteins.

In order to verify the experimental sensitivity of the new experiment, we acquired the proposed i(HCA)CO(CA)NH

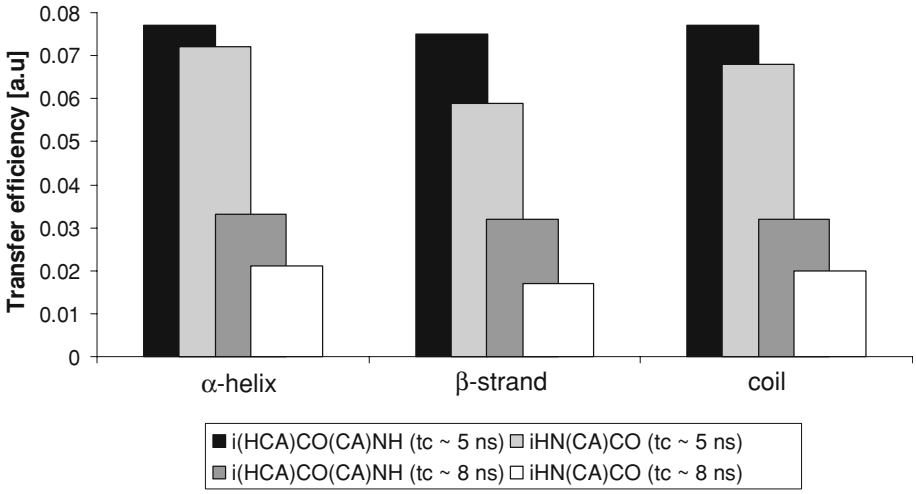

Fig. 2 Theoretical coherence transfer efficiencies for i(HCA)CO(CA)NH and intra-HN(CA)CO experiments in case of extended, α-helical, and random coil conformations. Calculations have been carried for two proteins having overall rotational correlation times τ_c of 5 and 8 ns. *Black* and *dark gray* (*light gray* and *white*) color coding correspond to transfer efficiencies for i(HCA)CO(CA)NH (intra-HN(CA)CO) on proteins with τ_c 5 and 8 ns, respectively

experiment and the intra-HN(CA)CO scheme with MQ implementation on human ubiquitin, a 8.6 kDa (76 residues) globular protein with the overall rotational correlation time (τ_c) of 4.5 ns at 296 K. Figure 3 shows two-dimensional $^{13}C'-^{1}H^{N}$ correlation maps from uniformly $^{15}N/^{13}C$ labeled ubiquitin, recorded with the proposed i(HCA)CO(CA)NH pulse sequence (panel a) and the non-TROSY implementation of the intra-HN(CA)CO scheme (panel b) using identical $t_{1,max}$ of 9.5 ms Comparison of attainable signal intensities for non-overlapping cross peaks between these two experiments, plotted as a function of amino acid residue in Fig. 4, reveals that a vast majority of the $^{1}H^{N}(i)-^{13}C'(i)$ cross peaks are more intense in the i(HCA)CO(CA)NH spectrum in comparison to the intra-HN(CA)CO spectrum. This holds true most prominently for cross-peaks stemming from residues in the α-helical and β-turn/hairpin conformations, or more precisely for residues having $^{2}J_{NC\alpha}$ coupling <7 Hz, indicative of polypeptide torsion psi (ψ) spanning from −50° to 50° (Puttonen et al. 2006). In those cases, sensitivity improvement by a factor of 1.5–3 can be realized (Fig. 4), whereas in the case of β-strand conformation, sensitivity improvement is smaller, 10–50%. Only in few exceptions, the sensitivity of intra-HN(CA)CO was slightly better than the proposed experiment. One possible explanation for this discrepancy is the presence of long-range carbon–carbon couplings (Hu and Bax 1996, 1997, 1998 Hennig et al. 1997, 2000), which modulate the detected signal amplitude by additional $\cos(2\pi JT_A)$ or $\cos(2\pi J(T_A + T_C + T_{CC}))$ term(s). In ubiquitin, this can be attributed at least to three glutamate residues, namely E16, E18 and E64 in which a three-bond coupling between Cα and carboxyl C′ modulates the signal during the long Cα → N transfer period between time point *a* and *d*. On the other hand, we realized that i(HCA)CO(CA)NH is also less prone to chemical exchange with solvent, yielding a clearly higher S/N for solvent exposed amides (e.g. T9 and A46 in ubiquitin) in comparison to the "out-and-back" type intra-HN(CA)CO experiment. In summary, on average a sensitivity gain of 1.65 was obtained in ubiquitin when using the i(HCA)-CO(CA)NH experiment for establishing the intraresidual H–N–C′ correlations (Fig. 4).

In addition to increased sensitivity, the proposed i(HCA)CO(CA)NH experiment offers significantly higher resolution in the $^{13}C'(t_1)$ dimension in comparison to the intra-HN(CA)CO scheme. The latter limits the attainable resolution to ~9–10 ms owing to significant time required for out- and back $^{13}C^{\alpha} \rightarrow {}^{13}C' \rightarrow {}^{13}C^{\alpha}$ transfer in relation to the overall duration of the constant-time period (CT ~ 28 ms). Acquisition time of 9–10 ms in the t_1 domain is too short for certain applications, especially for the backbone assignment of intrinsically disordered proteins, resulting in sparse resolution in the $^{13}C'$ dimension albeit accidental cross peak overlap is diminished owing to pure intraresidual transfer. Nevertheless, effective experimental resolution in the $^{13}C'$ dimension of the i(HCA)-CO(CA)NH spectrum can at least be doubled with respect to the intra-HN(CA)CO utilizing the MQ implementation.

Enhanced resolution obtained using the i(HCA)CO (CA)NH scheme is most appropriately illustrated in Fig. 3c, showing a two-dimensional $^{1}H^{N}(i)-^{13}C'(i)$ correlation map of ubiquitin recorded with the i(HCA)CO(-CA)NH experiment using a $t_{1,max}$ of 19 ms. It can be readily appreciated by comparing the attainable resolution between spectra in Fig. 3a–c that the proposed intraresidual i(HCA)CO(CA)NH sequence offers a significant resolution enhancement along the $^{13}C'$ domain in comparison to the intra-HN(CA)CO scheme.

Final point of interest concerns phase properties of emerging cross peaks in the i(HCA)CO(CA)NH spectrum. Glycines are in opposite phase with respect to those of the other amino acids in the original (HCA)CO(CA)NH experiment (Löhr and Rüterjans 1995). As magnetization transfer from Cα to N takes places during the period of

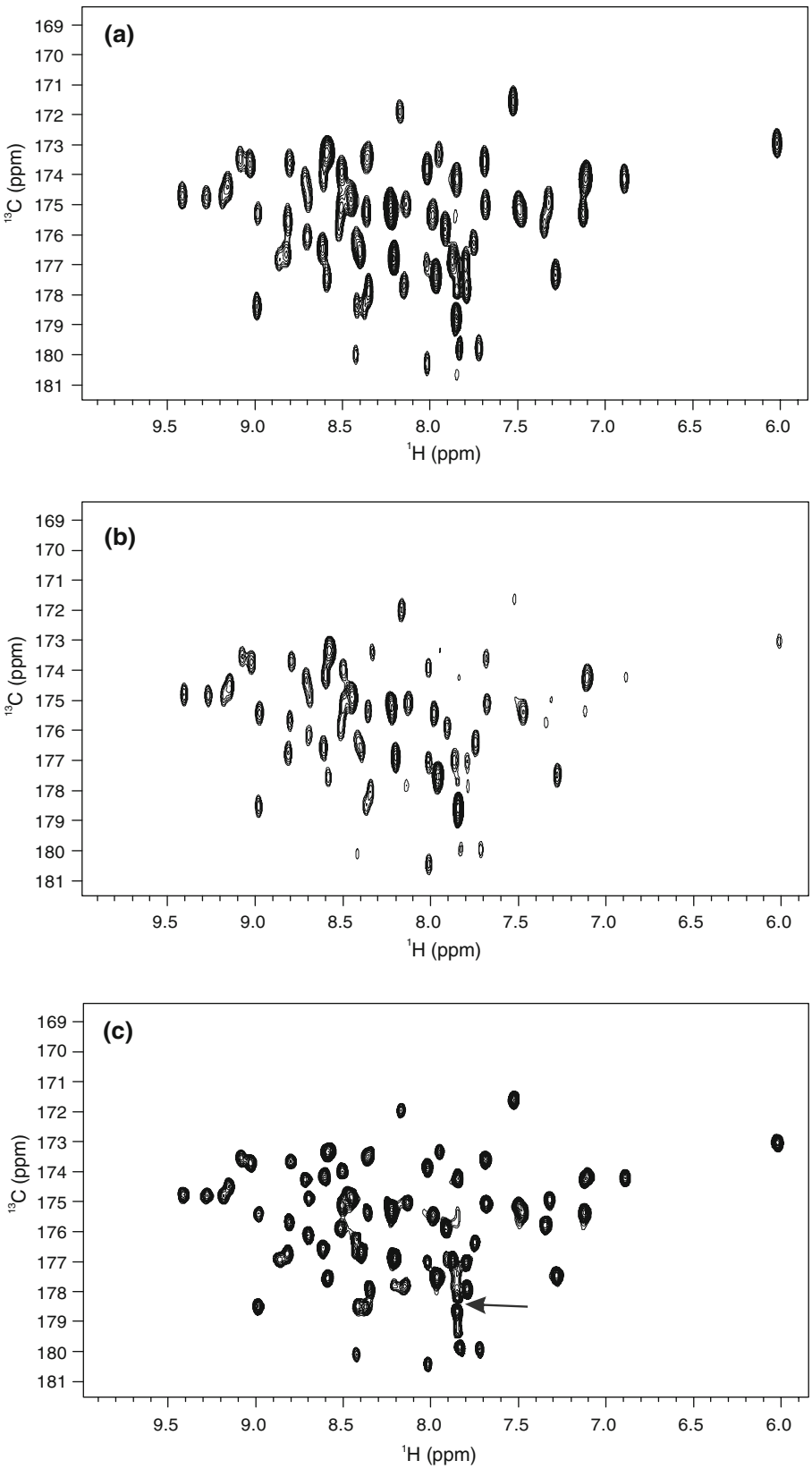

Fig. 3 Two-dimensional $^{13}C\prime-^{1}H^{N}$ correlation spectra of human ubiquitin, acquired with the i(HCA)CO(CA)NH (Fig. 1a) and a non-TROSY analog of the intra-HN(CA)CO experiments (Nietlispach 2004) without t_2 (^{15}N) incrementation. *Panels* **a** and **c** show i(HCA)CO(CAN)H spectra recorded with 19 (32 transients) and 38 (16 transients) t_1 increments, corresponding to acquisition times of 9.5 and 19 ms, respectively. The intra-H(NCA)CO spectrum, recorded under identical experimental conditions to the spectrum in *panel* **a** is displayed in *panel* **b**. Positive and negative contours are drawn without distinction. The *arrowhead* in *panel* **b** points to crosspeak corresponding to C-terminal G76 which is 90° out of phase with respect to other signals. Spectra were processed using identical weighting functions and data matrix sizes, and are shown with identical contour levels, using a spacing factor of 1.2. All spectra were acquired from a 1.9 mM sample of human ubiquitin on a Varian INOVA 600 MHz NMR spectrometer. Total experimental time for each spectrum was 24 min

$\sim 1/(2J_{C\alpha C\beta})$ ($\sim$57 ms), the sign information regarding Gly residues is lost. This can be compensated for by setting delay τ_2 to 4.4 ms instead of traditional 2.4 ms. As a result, the transfer factor $\sin(\pi J_{C\alpha H\alpha}\tau_2)\cos(\pi J_{C\alpha H\alpha\tau 2})$ for glycines will be negative, reintroducing sign properties of the original (HCA)CO(CA)NH scheme. A closer inspection of i(HCA)CO(CA)NH spectra in Fig. 3a, c reveals that the cross peak stemming from the C-terminal residue shows phase distortion with respect to other signals. This 90° phase difference originates from the N(i)–Cα(i)–C′(i) spin system at the carboxyl terminus. There is no ^{15}N spin at the ($i + 1$) position i.e. the pulse phase setting selects the $\sin(\omega_{C'}t_1)$ modulated signal after the t_1 period, whereas the $\cos(\omega_{C'}t_1)$ modulated signal is selected for remainder of residues.

Application to the assignment of intrinsically unfolded protein CT16

Intrinsically unfolded proteins are notoriously difficult to assign due to poorly dispersed chemical shifts of protons as well as aliphatic carbons, rendering the traditional assignment protocols based on Cα and Cβ chemical shifts inefficient (Yao et al. 1997). On the contrary, the carbonyl carbon chemical shift, containing contributions from the succeeding residue also, is a very useful aid for the assignment of unstructured regions in proteins (Dyson and Wright 2001; Sayers and Torchia 2001). As a real benchmark, we applied the i(HCA)CO(CA)NH experiment for the assignment of the 112-residue cancer/testis antigen PAGE5 also called CT16. According to NMR data, CT16 is highly disordered as manifested by poor ^{1}H chemical shift dispersion. Indeed, sequential assignment of CT16, based on ^{13}Cα and ^{13}Cβ chemical shift failed despite using unidirectional iHNCACB and HN(CO)CACB experiments, which minimize the emergence of accidental resonance overlap. This is most distinctly illustrated in Fig. 5a, showing highly degenerate ^{13}Cα and ^{13}Cβ chemical shifts for three glutamates in the iHNCACB experiment. However, using the i(HCA)CO(CA)NH and HNCO experiment pair, the multitude of solutions encountered in the iHNCACB/HN(CO)CACB spectra was readily unraveled as demonstrated in Fig. 4b. Excerpts of highly resolved two-dimensional planes of i(HCA)CONH and HNCO are shown in Fig. 4c, exemplifying the 'sequential walk' obtained by employing unidirectional i(HCA)CO (CA)NH/HNCO experiments to the assignment of CT16. Using this approach, we obtained a nearly complete (>91%) sequence-specific assignment of

Fig. 5 The i(HCA)CO(CA)NH/HNCO experiment pair was used to resolve ambiguities in the sequential assignment of CT16. **a** The HN(CO)CACB strip shows the α/β shifts of the residue previous to D83. Chemical shift degeneracy results in three possible solutions for E82 in the iHNCACB spectrum. **b** Only the second i(HCA)CONH strip has a C′ chemical shift matching to that of E82 shown in the HNCO, the two others corresponding to those of E35 and E55. **c** 'Sequential walk' by employing i(HCA)CO(CA)NH/HNCO experiments for the assignment of residues V64–T67 of CT16 ▶

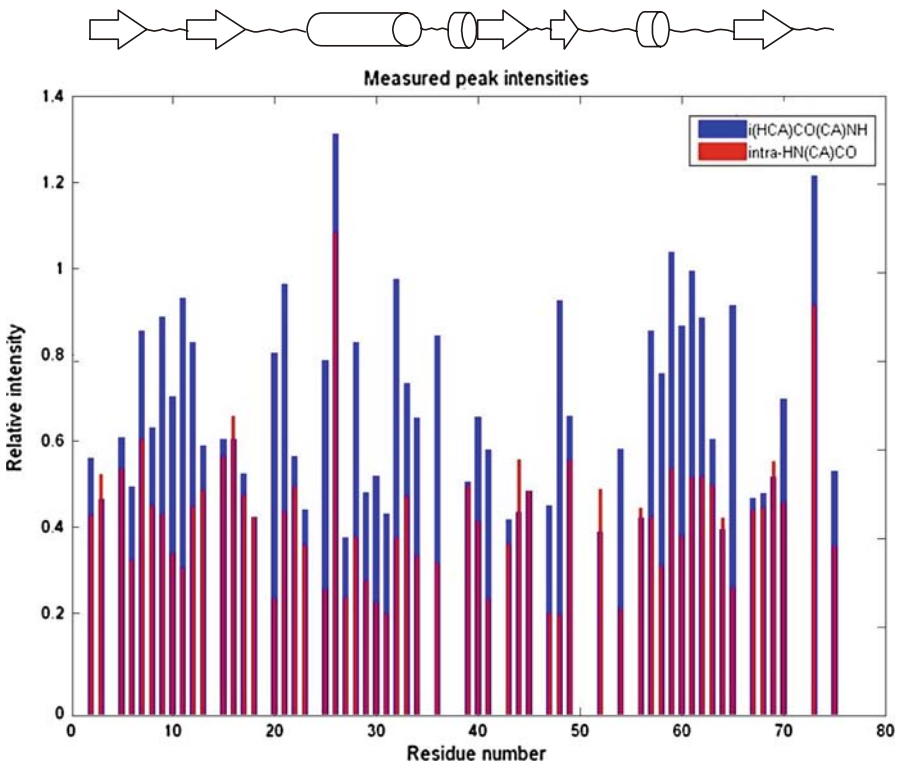

Fig. 4 Comparison of attainable crosspeak heights between i(HCA)CO(CA)NH (*blue bars*) and intra-HN(CA)CO (*red bars*) spectra plotted as a function of ubiquitins amino acid sequence. Secondary structure elements found in ubiquitin are displayed above the *plot* area

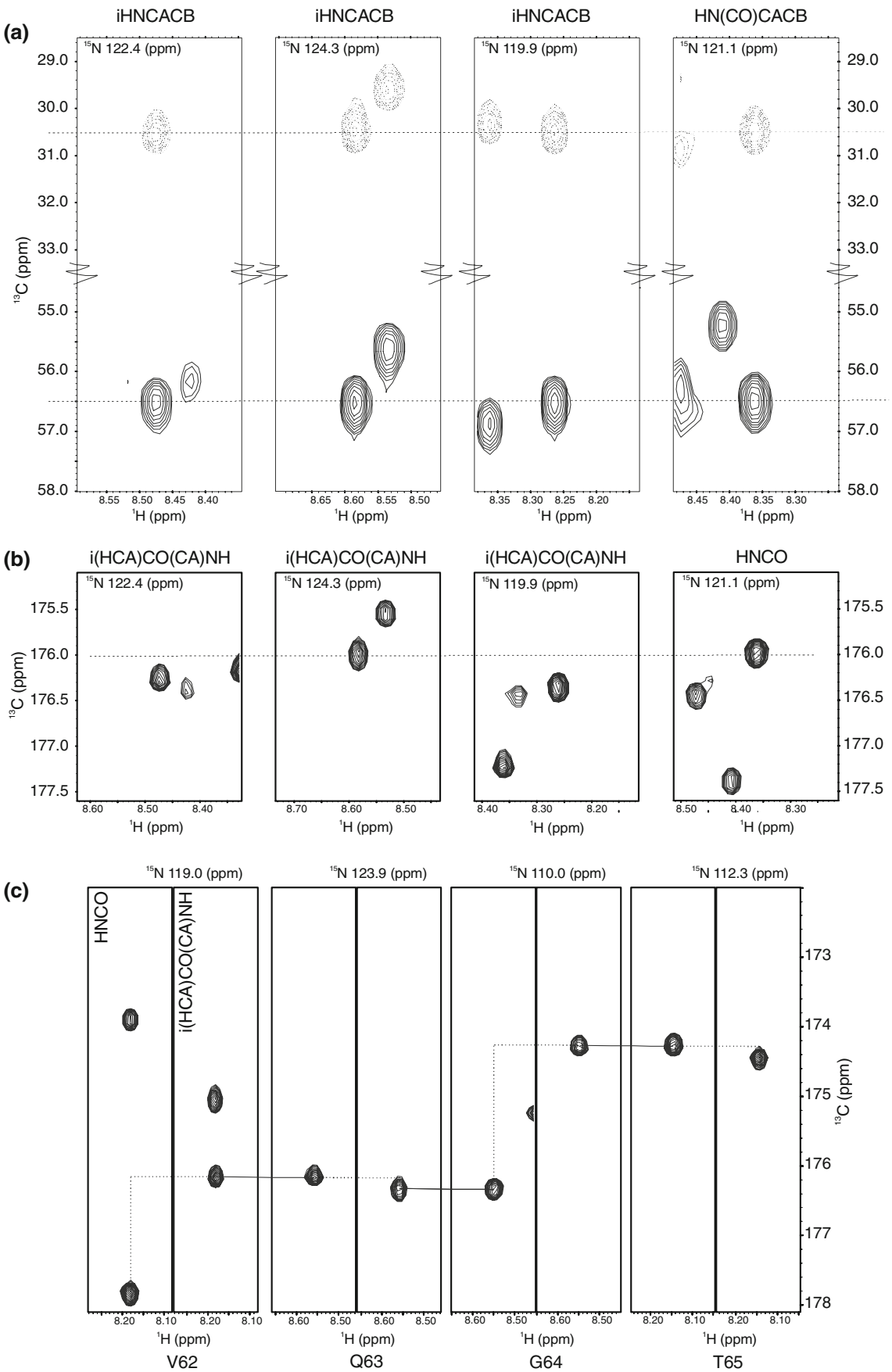
(a)
iHNCACB
iHNCACB
iHNCACB
HN(CO)CACB
15N 122.4 (ppm)
15N 124.3 (ppm)
15N 119.9 (ppm)
15N 121.1 (ppm)
13C (ppm)
1H (ppm)
(b)
i(HCA)CO(CA)NH
i(HCA)CO(CA)NH
i(HCA)CO(CA)NH
HNCO
15N 122.4 (ppm)
15N 124.3 (ppm)
15N 119.9 (ppm)
15N 121.1 (ppm)
13C (ppm)
1H (ppm)
(c)
15N 119.0 (ppm)
15N 123.9 (ppm)
15N 110.0 (ppm)
15N 112.3 (ppm)
HNCO
i(HCA)CO(CA)NH
13C (ppm)
1H (ppm)
V62
Q63
G64
T65

HN, N, C′, Cα and Cβ resonances for non-proline residues (102) in CT16, missing assignment originating from few N-terminal residues (G1–H6 and S10–S13) with rapidly exchanging amide protons, whose signal were not detectable in ^{15}N-HSQC spectrum either.

Conclusions

Sequential assignment strategy based on ^{13}C′ chemical shift is invaluable especially in the case of intrinsically unfolded proteins, where degeneracy of ^{13}Cα/^{13}Cβ shifts severely impedes both automated and manual assignment of main-chain resonances. We have introduced a new unidirectional i(HCA)CO(CA)NH scheme for ^{15}N/^{13}C labeled proteins, which improves both sensitivity and resolution of *intraresidual* H(*i*)–N(*i*)–C′(*i*) correlations in comparison to the out-and-back type intra-HN(CA)CO experiment. Sensitivity of the i(HCA)CO(CA)NH experiment was found to be on average ~1.65 higher than the non-TROSY version of the MQ intra-HN(CA)CO on a small globular protein. Moreover, experimental resolution can be extended from 10 to 24 milliseconds in the ^{13}C′ dimension, which is highly desired especially in the case of natively unfolded proteins. Experiments utilizing ^{13}C′ chemical shift for establishing sequential connectivities are of key importance for the assignment of intrinsically unfolded proteins such as CT16 which was used as an example in this work. A nearly complete main-chain assignment of the 112-residue, natively unfolded protein was obtained together with the conventional HNCO experiment demonstrating that the i(HCA)CO(CA)NH experiment is very powerful method for resolving ambiguities in the assignment of ^{15}N/^{13}C labeled proteins. We therefore have every reason to believe that the proposed unidirectional i(HCA)CO(CA)NH experiment can be put into good use in the assignment of ^{15}N/^{13}C-labeled proteins.

Materials and methods

The proposed i(HCA)CO(CA)NH experiment and a non-TROSY version of the intra-HN(CA)CO with a constant time MQ implementation (Nietlispach 2004) were recorded on 1.9 mM uniformly ^{15}N, ^{13}C labeled human ubiquitin having a molecular mass of 8.6 kDa (76 residues), dissolved in 95/5% H_2O/D_2O, 10 mM potassium phosphate buffer (pH 5.8) in a sealed Wilmad 535PP NMR tube at 20°C. Spectra shown in Fig. 3a were recorded on a Varian Unity INOVA 600 NMR spectrometer, equipped with a ^{15}N/^{13}C/^{1}H triple-resonance probehead and an actively shielded *z*-axis gradient system. For sensitivity and resolution comparison purposes with respect to the intra-HN(CA)CO experiment on human ubiquitin, both three-dimensional i(HCA)CO(CA)NH and intra-HN(CA)CO experiments were run as two-dimensional ^{13}C′–^{1}H correlation experiments. Intraresidual i(HCA)-CO(CA)NH spectra shown in Fig. 3a, c were acquired using 32/16 transients per FID with 19/38 and 1,024 complex points, corresponding to acquisition times of 9.5/19 and 85 ms in t_1 and t_3, respectively. Intraresidual HN(CA)CO spectrum in Fig. 3b was collected with parameters identical to those used for i(HCA) COCA)NH spectrum in Fig. 3a. Total acquisition time for each experiment was 24 min. Spectra were processed and analyzed using the standard VNMRJ 2.1 revision B software package (Varian associates 2006). Prior to zero-filling to 1,024 × 4,096 data matrix, followed by the Fourier transform, the data were weighted with a shifted squared sine-bell functions applied to both dimensions.

For the assignment of 0.8 mM uniformly ^{15}N/^{13}C CT16 (110 residues), dissolved in 93/7% H_2O/D_2O, 10 mM Tris–HCL (pH 7.5), 50 mM NaCl in a Shigemi microcell at 25°C, the proposed i(HCA)CO(CA)NH scheme together with iHNCACB (Tossavainen and Permi 2004), HN(CO)CACB (Yamazaki et al. 1994) and HNCO experiments (Muhandiram and Kay 1994) was employed. The measurements were carried out on a Varian Unity INOVA 800 NMR spectrometer, equipped with a conventional ^{15}N/^{13}C/^{1}H triple-resonance probehead and an actively shielded *xyz*-axis gradient system. For i(HCA)CO(CA)NH 52, 52 and 682 complex points in t_1, t_2, and t_3 were collected, respectively. These correspond to acquisition times of 17.3, 23.6, and 85.2 ms in ^{13}C′, ^{15}N and ^{1}H dimensions, respectively. Two transients per FID were used for signal accumulation, resulting in a total experimental time of 7.3 h.

Acknowledgments This work was financially supported by the grants 120062, 122170, and 131144 (to P. P.) from the Academy of Finland. We thank Anne Hakonen for excellent technical assistance.

References

Alho N, Klaavuniemi T, Ylanne J, Permi P, Mattila S (2007) Backbone NMR assignment of the internal interaction site of ALP. Biomol NMR Assign 1:85–87

Bazzo R, Cicero DO, Barbato G (1996) A new three-dimensional pulse sequence for correlating intraresidue NH, N, and CO chemical shifts in ^{13}C, ^{15}N-labeled proteins. J Magn Reson B 110:65–68

Bendall MR (1995) Heteronuclear J coupling precession during spin-lock and adiabatic pulses. Use of adiabatic inversion pulses in high-resolution NMR. J Magn Reson A116:46–58

Bersch B, Rossy E, Coves J, Brutscher B (2003) Optimized set of two-dimensional experiments for fast sequential assignment, secondary structure determination, and backbone fold validation of ^{13}C/^{15}N-labelled proteins. J Biomol NMR 27:57–67

Brutscher B (2002) Intraresidue HNCA and COHNCA experiments for protein backbone resonance assignment. J Magn Reson 156:155–159

Clubb RH, Thanabal V, Wagner G (1992) A constant-time three-dimensional triple-resonance pulse scheme to correlate intraresidue 1HN, 15N, and 13C′ chemical shifts in 15N–13C-labelled proteins. J Magn Reson 97:213–217

Delaglio F, Torchia DA, Bax A (1991) Measurement of 15N–13C J couplings in staphylococcal nuclease. J Biomol NMR 1:439–446

Dyson HJ, Wright PE (2001) Nuclear magnetic resonance methods for elucidation of structure and dynamics in disordered states. Methods Enzymol 339:258–270

Folmer R, Otting G (2000) Sensitivity enhancement in (HCA)CONH experiments. J Biomol NMR 16:229–233

Griffey RH, Redfield AG (1987) Proton-detected heteronuclear edited and correlated nuclear-magnetic-resonance and nuclear Overhauser effect in solution. Q Rev Biophys 19:51–82

Grzesiek S, Bax A (1992) Improved 3D triple-resonance NMR techniques applied to a 31-kDa protein. J Magn Reson 96: 432–440

Hennig M, Ott D, Schulte P, Lowe R, Krebs J, Vorherr T, Bermel W, Schwalbe H, Griesinger C (1997) Determination of homonuclear 13C–13C J couplings between aliphatic carbon atoms in perdeuterated proteins. J Am Chem Soc 119:5055–5056

Hennig M, Bermel W, Schwalbe H, Griesinger C (2000) Determination of psi torsion angle restraints from $^{3}J(C_{\alpha}, C_{\alpha})$ and $^{3}J(C_{\alpha}, H^{N})$ coupling constants in proteins. J Am Chem Soc 122:6268–6277

Hu JS, Bax A (1996) Measurement of three-bond 13C–13C J couplings between carbonyl and carbonyl/carboxyl carbons in isotopically enriched proteins. J Am Chem Soc 118:8170–8171

Hu JS, Bax A (1997) Determination of ϕ and x1 angles in proteins from ^{13}C–^{13}C three-bond J couplings measured by three-dimensional heteronuclear NMR. How planar is the peptide bond? J Am Chem Soc 119:6360–6368

Hu JS, Bax A (1998) Measurement of three-bond, 13C′-13Cb J couplings in human ubiquitin by a triple resonance, E.COSY-type NMR technique. J Biomol NMR 11:199–203

Jaravine VA, Zhuravleva AV, Permi P, Ibraghimov I, Orekhov VY (2008) Hyperdimensional NMR spectroscopy with nonlinear sampling. J Am Chem Soc 130:3927–3936

Jiang L, Coggins BE, Zhou P (2005) Rapid assignment of protein side chain resonances using projection-reconstruction of (4, 3)D HC(CCO)NH and intra-HC(C)NH experiments. J Magn Reson 175:170–176

Kay LE, Ikura M, Tschudin R, Bax A (1990) Three-dimensional triple-resonance NMR spectroscopy of isotopically enriched proteins. J Magn Reson 89:496–514

Kay LE, Keifer P, Saarinen T (1992) Pure absorption gradient enhanced heteronuclear single quantum correlation spectroscopy with improved sensitivity. J Am Chem Soc 114:10663–10665

Kupće E, Wagner G (1995) Wideband homonuclear decoupling in protein spectra. J Magn Reson 109A:329–333

Lescop E, Schanda P, Rasia R, Brutscher B (2007) Automated spectral compression for fast multidimensional NMR and increased time resolution in real-time NMR spectroscopy. J Am Chem Soc 129:2756–2767

Löhr F, Rüterjans H (1995) A New triple-resonance experiment for the sequential assignment of backbone resonances in proteins. J Biomol NMR 6:189–197

Marion D, Ikura M, Tschudin R, Bax A (1989) Rapid recording of 2D NMR-spectra without phase cycling—application to the study of hydrogen-exchange in proteins. J Magn Reson 85:393–399

Muhandiram DR, Kay LE (1994) Gradient-enhanced triple-resonance NMR experiments with improved sensitivity. J Magn Reson B103: 203–216

Nietlispach D (2004) A selective intra-HN(CA)CO experiment for the backbone assignment of deuterated proteins. J Biomol NMR 28:131–136

Nietlispach D, Ito Y, Laue ED (2002) A novel approach for the sequential backbone assignment of larger proteins: selective intra-HNCA and DQ-HNCA. J Am Chem Soc 124:11199–11207

Permi P (2002) Intraresidual HNCA: an experiment for correlating only intraresidual backbone resonances. J Biomol NMR 23:201–209

Permi P, Annila A (2004) Coherence transfer in proteins. Prog Nucl Magn Reson Spectr 44:97–137

Puttonen E, Tossavainen H, Permi P (2006) Simultaneous determination of one- and two-bond scalar and residual dipolar couplings between $^{13}C'$, $^{13}C^{\alpha}$, and ^{15}N spins in proteins. Magn Reson Chem 44:168–176

Sattler M, Schleucher J, Griesinger C (1999) Heteronuclear multidimensional NMR experiments for the structure determination of proteins in solution employing pulsed field gradients. Prog Nucl Magn Reson Spectr 34:93–158

Sayers EW, Torchia DA (2001) Use of the carbonyl chemical shift to relieve degeneracies in triple-resonance assignment experiments. J Magn Reson 153:246–253

Shaka AJ, Lee CJ, Pines A (1988) Iterative schemes for bilinear operators—application to spin decoupling. J Magn Reson 77: 274–293

Silver MS, Joseph RJ, Hoult DI (1984) Highly selective $\pi/2$ and π pulse generation. J Magn Reson 59:347–351

Tessari M, Gentile LN, Taylor SJ, Shalloway DI, Nicholson LK, Vuister G (1997) Heteronuclear NMR studies of the combined Src homology domains 2 and 3 of pp60 c-Src: Effects of phosphopeptide binding. Biochemistry 36:14561–14571

Tossavainen H, Permi P (2004) Optimized pathway selection in intraresidual triple-resonance experiments. J Magn Reson 170: 244–251

Yamazaki T, Lee W, Arrowsmith CH, Muhandiram DR, Kay LE (1994) A suite of triple-resonance NMR experiments for the backbone assignment of ^{15}N, ^{13}C, ^{2}H labeled proteins with high-sensitivity. J Am Chem Soc 116:11655–11666

Yao J, Dyson HJ, Wright PE (1997) Chemical shift dispersion and secondary structure prediction in unfolded and partly folded proteins. FEBS Lett 419:285–289